

Received May 5, 2020, accepted June 1, 2020, date of publication June 5, 2020, date of current version June 18, 2020.

Digital Object Identifier 10.1109/ACCESS.2020.3000294

Helicopter Control During Landing on a Moving Confined Platform

SEBASTIAN TOPCZEWSKI^{ID}, JANUSZ NARKIEWICZ, AND PRZEMYSŁAW BIBIK

Division of Automation and Aeronautical Systems, Faculty of Power and Aeronautical Engineering, Warsaw University of Technology, 00-665 Warsaw, Poland

Corresponding author: Sebastian Topczewski (stopczewski@meil.pw.edu.pl)

ABSTRACT The paper presents a control algorithm for a helicopter automatic approach and landing on a moving confined platform. It discusses landing on a sea vessel deck as a representative case for a mobile confined area. The dynamic model of a single rotor helicopter with a control system, developed in the FLIGHTLAB environment, and validated against flight tests data, is used to investigate control efficiency. The developed control method is based on the Linear Quadratic Regulator combined with prediction of motion of the landing area. An important part of the research was analysis of availability of the data needed for controlling the rotorcraft. The simulations of approach and landing on a moving vessel in various environmental conditions confirmed the efficiency of the developed control methodology.

INDEX TERMS Helicopter automatic control, confined area landing, helicopter motion modeling, vessel motion prediction.

I. INTRODUCTION

Helicopters perform a variety of missions, very often operating in degraded environmental and visual conditions, which may affect flight safety. During many operations the helicopter approaches and lands on a confined area which may be solid (helipads on the ground or at tops of buildings, offshore platforms) and moving platforms (decks of vessels but also platforms on ground vehicles). In this research, an approach and landing on a sea vessel deck is studied as a representative mission, which contains all detrimental factors influencing helicopter performance and safety.

Landing on a confined, moving vessel deck area in adverse environmental conditions is a very complicated and demanding task for a pilot, as helicopter flight and handling qualities are influenced by several detrimental factors, such as:

- environmental conditions: variation of velocity and direction of wind, air gusts and turbulence, degraded visibility during day and operations at night,
- landing deck size and motion (translations and rotations),
- limitations from the helicopter flight envelope and helicopter handling and flying qualities.

These factors make helicopter landing on a vessel deck a challenging task for a pilot, who may be supported by technology.

The associate editor coordinating the review of this manuscript and approving it for publication was Rosario Pecora^{ID}.

Typically, flight and/or operation manuals include specific procedures, which provide guidance for safe operation in various conditions. However, development of automatic control systems (hardware and software including efficient control algorithms) which use data from modern, advanced sensors opens several opportunities to support the helicopter pilot during a mission.

Development of a helicopter automatic control system performing landing on a moving, confined platform must take into account several factors, such as dynamics of the helicopter itself and its control system, available data from sensors, control strategy, environmental conditions and vessel motion. An overview of literature reflecting solutions for these challenges is presented below.

Reference [1] describes a system for automatic landing of a Vertical Take Off and Landing (VTOL) type unmanned aerial vehicle on a moving ship deck using a camera and Inertial Navigation System (INS) data to determine the relative vessel helicopter position and to generate approach and landing trajectories.

In [2] a control algorithm augments the Stability Augmentation System (SAS) by adding more robustness for wind and gusts, which occur due to flow over vessel superstructures. The system is integrated with other helicopter control systems.

In [3] navigation and control of a helicopter in approach to landing is presented, focused on application of visual

navigation assuming lack of the Global Positioning System (GPS) signal, but also taking into account poor visibility conditions. A three-phase trajectory planner is developed, which uses models of a helicopter and vessel dynamics.

Reference [4] presents a concept of a helicopter control system for approaching a vessel. The authors take into account influences of the airwake on helicopter flight.

In [5] a system for autonomous landing is developed and implemented on a small unmanned helicopter. The automatic control system is composed of navigation and control modules (tracking and landing modes) and is adjusted for operation on a moving confined platform. Prediction of ship motion is implemented to establish the best landing moment.

Reference [6] presents the Model Predictive Control (MPC) of the helicopter-vessel operations in degraded weather conditions, using nonlinear helicopter and vessel dynamic models, and predicting vessel motion to optimize the landing phase. It investigates various airwake models acting on helicopter flight. The MPC control system design is evaluated for automatic landing of a helicopter on a vessel in sea state 5 and reposition of the helicopter during different wind conditions.

Robust MPC methodology developed for highly constrained helicopter flights including discontinuous flight trajectories is also shown in [7].

In [8] a navigation and control system is described for ship-board operations of an unmanned VTOL aircraft. The system has a modular structure with the function of estimating the deck motion.

Reference [9] presents a control algorithm for landing of the autonomous AVATAR helicopter. The system uses a GPS receiver for navigation and a vision camera for tracking the landing deck.

Reference [10] compares three automatic control techniques (Linear Quadratic Integral (LQI), Model Predictive Control (MPC) and Loop-Shaping Design (LSD)) for vessel-helicopter operations, applied to nonlinear helicopter and vessel dynamic models.

Reference [11] presents a CTM – Compensatory Tracking Model algorithm used for flight along a specified trajectory. An algorithm is implemented in the FLIGHTLAB environment and it is used to study actions necessary for helicopter take-off and landing on a moving vessel when there are airwake and turbulence.

In [12] an optical flow method is used for automatic control of a helicopter during landing on a vessel. The optical flow parameter for helicopter guidance is similar to a pilot typical control strategy. The computation results were evaluated using the Bell 412HP dynamic model implemented in the FLIGHTLAB environment.

In [13] a planner for helicopter landing on a stationary confined area is developed taking into account approach procedures, helicopter dynamic limitations, presence of obstacles and restrictions of airspace areas.

Reference [14] presents a precision landing method via trajectory planning taking into account landing area obstacles.

The authors focused on various aspects of confined landings like approach and landing strategy, and landing site selection. In this concept for trajectory and landing point selection, system data from helicopter INS, GPS and LIDAR sensors are used for navigation.

Reference [15] develops an optimal controller and trajectory planner (based on Variational Hamiltonian and Euler-Lagrange equations) designed for tracking and landing on a moving platform. The reduced helicopter kinematic model is used to derive an optimal controller.

Reference [16] presents a vision-based landing system for helicopter-ship operations. The states of the ship motion are estimated using Kalman filtering. The landing is decomposed into three phases. In the first phase a ship is searched and detected by a visual system using fuzzy logic algorithms. Next the ship is tracked by the helicopter on-board system. The tracking is formulated as Bayesian estimation and solved using a Kalman filter. Finally, automatic landing is performed using a PI controller.

Helicopter landing guidance using Model Predictive Path Integral (MPPI) is presented in [17] as a further development of research presented in [18]. It is a stochastic optimum control method which was used to calculate control inputs using the model of vehicle dynamics. In the paper a six DOF linear model of the helicopter is used to predict its motion while landing and a nonlinear model is used as a representation of an actual helicopter state. A ship deck motion model is a representative of a selected type of vessel based on statistical data. The authors present several test cases in which they have evaluated performance of MPPI method and utility of using linear models for prediction in the case of a helicopter landing on a vessel deck.

The confined area landing is also considered for prospective Personal Aerial Vehicles (PAV) operations [19]–[21]. In [22] the authors assumed that PAV is positioned in a hover directly over a confined landing area and by vertical descent achieves the target landing point.

As a summary of this literature review (far from being complete or comprehensive), it may be stated that various methods and models are used for solving the problem of safe and efficient landing on a moving platform. The majority of research is done by simulations, placing emphasis of selected aspects of the mission (trajectory planning, navigation, control, predicting deck motion).

The research presented in this paper responds to a practical need of a holistic approach to complete control system development, used for automatic approach and landing on a moving vessel deck, which takes into account available sensor data, requirements for trajectory planning also according to the published procedures and simplicity of computation to be applicable in real time.

The novelty of our approach is development of the integrated control system composed of an automatic control and a prediction algorithm which may be used for an approach and landing of a helicopter on a moving confined area in various environmental conditions, reducing the risk in comparison to



FIGURE 1. Leonardo PZL SW-4 helicopter.

manned, non-automatic operations. The system can be also used in research, to define which navigation data is necessary to successfully perform this task and to compare procedures of landing operations in various environmental conditions to define approach and landing times.

In the following text the helicopter model will be described and necessary sensor data availability will be discussed followed up by a description of control methodology and algorithm for prediction of vessel deck motion. The efficiency of software will be validated, in terms of applicability in a simulator as the next step of the project.

II. HELICOPTER MODEL

The helicopter simulation model was developed in the FLIGHTLAB software environment, which is well established standard in industry, research and academia. The various aspects of rotorcraft modelling are developed there, taking into account the variety of models of dynamics, aerodynamics, structures and control systems [23]. Despite the convenience of modelling, the efficient FLIGHTLAB application requires expertise in rotorcraft aeromechanics for proper selection of the models of loads and validation of model results by flight test data. The model selected in this research reflects the PZL SW-4 helicopter configuration (Fig. 1). It is a single rotor helicopter powered by one turboshaft engine with a fully articulated main rotor and a see-saw tail rotor. The main rotor is a three-bladed, articulated rotor with flap, lag and pitch hinges sequence. The main rotor rotates clockwise (looking from above), and the tail rotor rotates clockwise looking from the left side (the lower blade is advancing). The simulation model consists of a fuselage, a main rotor, a tail rotor, an empennage (central vertical stabilizer, two small vertical stabilizers and two symmetrical horizontal stabilizers), an engine and an undercarriage. All parts of a helicopter are modeled as rigid. Loads of the main and tail rotors are computed using blade element theory. The aerodynamic loads are calculated using the model of quasi-steady aerodynamic flow with stall delay, and Peters-He 6 state model of induced velocity for the main rotor and one state for the tail rotor. The aerodynamic loads on the fuselage and on the empennage are calculated using

look-up tables of empirical airfoils data; interaction of main rotor-fuselage is also taken into account. The engine power is calculated using a FLIGHTLAB model of a turboshaft engine.

The model of the helicopter control system contains hydraulic boosters in the control line between the pilot stick and the swashplate. Besides the manual control system, the helicopter model contains automatic control with four electromechanical actuators. The controls of the main and tail rotors are modelled as ideal ones, i.e., the adequate actuator forces are always generated to produce the swashplates motions for the required changes of rotor blades pitch angles.

The simulation model includes 35 states:

- Helicopter fuselage (12 states) – helicopter position (3), velocities (3), roll, pitch and yaw angles (3), roll, pitch and yaw rates (3),
- Main rotor (18) – induced velocity (6) – uniform, 0th harmonic, 1st harmonic (cos), 1st harmonic (sine), 2nd harmonic (cos), 2nd harmonic (sine), each blade flap (3) and lag (3) angles, and each blade flap (3) and lag (3) rates,
- Tail rotor (3) – mean induced velocity (1), teetering angle (1), teetering rate (1),
- Propulsion (2) – shaft angle (1), shaft rate (1).

The helicopter model in FLIGHTLAB software environment consists of several hierarchical, integrated elements described here for completeness:

- Environment

The atmosphere is modeled using a function which is based on the Air Research and Development Command Model Atmosphere. This model is based on hydrostatic equation and ideal gas law. The output of the model is: ambient temperature, pressure, air density and speed of sound at the flight level.

- Main rotor

The main rotor is articulated. The blades are mounted to the hub by three hinges: flap, lag and pitch, in order from the axis of the shaft. The blades are described by: the shape (chord, radius, position of the pitch axis), geometric twist assumed to be linear along the blade, mass distribution, position of the centers of mass of the blade elements relative to the pitch axis, and distribution of mass inertia moments.

The airloads are modeled as nonlinear unsteady. The airfoil aerodynamic data tables consisting of coefficients of lift, drag and pitch moment are used, which depend on the angle of attack and local Mach number. Two-dimensional aerodynamic blade element method is used, that produces airloads as nonlinear functions of dynamic pressure, angle of attack and Mach number. Dynamic stall effects are included in the dynamic model – dynamic stall equations are described in terms of circulation related quantities which provide the airfoil dynamic stall loads.

The induced velocity is modeled as Peters-He six state inflow. The distribution of induced inflow at the rotor plane is described in terms of a set of harmonic and radial shape

functions as modal inflow states. For a current helicopter motion, induced velocity, local flow velocity components, angle of attack and Mach number are computed for each blade element.

- Tail rotor

The tail rotor is a teetering type. The inertia and aerodynamic loads are calculated using blade element method. The airloads are modeled as nonlinear unsteady in the same manner as at the main rotor. Induced velocity is modeled as Peters-He finite state.

- Fuselage

The fuselage is modeled as a 6 DOF rigid body. Its mass properties cover total mass, position of the center of mass and full inertia matrix. The fuselage airloads are modeled using empirical data for aerodynamic loads on a three dimensional body, which are functions of the angle of attack and angle of sideslip. The wind and the inflow velocity of the main rotor are taken into account in calculating angles of attack and slip. The data tables consisting of lift, side force, drag, roll, pitch and yaw moment coefficients are used. Two types of data tables can be distinguished here – for low and high angles of attack and sideslip. An aerodynamic side force, roll and yaw pitch moment coefficients are computed using interpolation of the function of the sideslip angle and angle of attack.

- Empennage

The central vertical stabilizer, two small vertical stabilizers and two symmetrical horizontal stabilizers are modeled. The empennage airloads are modeled as nonlinear functions of dynamic pressure, angle of attack and Mach number. Data tables consisting of aerodynamic coefficients are used.

- Undercarriage – skids

The landing gear system model consists of left and right skids and a tail skid. All landing gear is modeled using a full nonlinear spring/damper formulation. The landing gear model also considers ground friction.

- Propulsion

The helicopter model includes the propulsion system i.e. turboshaft engine and its dynamics. The propulsion system model consists of a set of components modeling the engine and transmission. The main propulsion subsystems cover inlet, compressor, combustor, gas turbine, power turbine, exhaust, shaft, clutch and gearbox within a FLIGHTLAB modeling block.

- Flight control system (hardware)

There are four control variables: main rotor collective and two cyclic (longitudinal and lateral) pitch angles and tail rotor collective pitch angle.

The helicopter dynamic simulation model was tuned and validated using flight test data received from the manufacturer covering both steady flight and dynamic response cases.

Referring to mathematical description, the helicopter model may be defined in a general form as:

$$\dot{x} = f(x, u, t) \quad (1)$$

The states x and control variables u were defined above. The right hand side of the equation are the complex expressions combining both analytical calculations as well as table look-up procedures. They are composed automatically by the software.

III. SENSOR DATA AVAILABILITY

Due to prospective application of the control algorithm in flight control system software, data available from sensors were analyzed. Two sets of data were considered – data collected on helicopter board and data which may be provided to the aircraft from outside.

Helicopter on-board systems may contain an INS/GPS integrated sensor providing measurements of all three components of helicopter position, linear velocity, linear acceleration, attitude and angular velocity. A similar data set may be measured for a ship deck using the same type of sensors, and transferred via a data link to the helicopter. The weather station on-board the vessel may measure wind direction and velocity. The Air Data Computer provides the airspeed, slip angle and angle of attack of the helicopter. The precise height above the landing deck, useful in the final landing phase, may be measured using a radioaltimeter on the helicopter.

There may also be other more sophisticated sensor systems and data fusion algorithms for obtaining the data needed for helicopter control, like for instance visual navigation methods, lidar or external helicopter radiolocation systems [24], [25]. The future systems are intended to support fully autonomous operations and all necessary data would be gathered and processed onboard a helicopter.

Sensor availability analysis proved that the input data required for the control method developed in this study are available even with a simple, commonly used helicopter on-board navigation system.

IV. HELICOPTER APPROACH AND LANDING STRATEGY

Helicopter landing on a vessel deck may be performed according to a recommended procedure. Six most common Dutch/British navy helicopter-vessel operating procedures (approach, take-off and landing) are described in [26].

In this research the landing operation is decomposed into three phases: approach to a moving landing deck, hovering relative to the deck and final landing with touchdown.

During the approach phase, the helicopter moves towards the position of hovering over the landing deck. The trajectory of the helicopter in this phase is prescribed by way points, and may describe any approach procedure required by regulations. A helicopter, controlled by LQR, passes through the prescribed waypoints with assumed error thresholds (this can be done with time points restrictions as well [27]). The start of the approach phase is also the beginning of collecting data of the vessel motion for a prediction algorithm (based on the autoregressive method) of the vessel motion. The approach phase is completed when the helicopter reaches the hovering position relative to the landing deck. During the next phase of operation, the helicopter hovers at a prescribed (safe) height

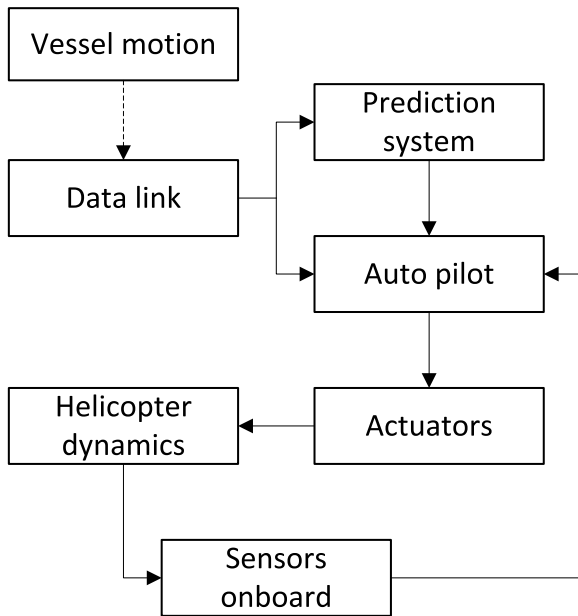


FIGURE 2. Control system – information flow.

over the landing deck. The prediction algorithm continues predicting the future deck position with a specified lead time. It is checked whether at the predicted touchdown moment the predicted pitch and roll angles of the vessel deck and relative vertical touchdown velocity (which is the sum of the helicopter and deck velocities) will not exceed the maximal allowable values.

The decision of starting the final landing phase is undertaken when the prediction system confirms that vertical touchdown velocity and pitch and roll angles of the vessel will not exceed the safe values. The final landing phase is performed automatically by the LQR controller.

A. AUTOMATIC FLIGHT CONTROL

Information flow of the control system is shown in Fig. 2. It is assumed that all phases of helicopter flight are performed automatically.

For flight control the Linear Quadratic Regulator (LQR) was selected and implemented.

The crucial elements of the LQR method are:

- linear continuous state-space system written as:

$$\dot{x} = Ax + Bu \quad (2)$$

where A is a state matrix and B is a control matrix,

- cost function:

$$J = \int_0^{\infty} (x^T Qx + u^T Ru) dt \quad (3)$$

where Q is a symmetrical, positively semi-defined state weight matrix and R is a symmetrical, positively defined control weight matrix,

- control feedback:

$$u = -K * (x - x_d) \quad (4)$$

where x is a vector of state variables, x_d is a vector of the desired values of state variables, u is a control vector, K is the feedback gain,

- feedback gain:

$$K = R^{-1} B^T P \quad (5)$$

where P is the matrix solution of the Riccati's equation,

- Riccati's equation:

$$A^T P + PA - PBR^{-1}B^T P + Q = 0 \quad (6)$$

Final procedure of the LQR operation is as follows:

- State space matrices A and B and weight matrices Q and R are followed to procedure which solve Riccati's equation.
- Using calculated P , gain matrix K is computed.
- Finally, using K matrix and the difference between current and desired state variables, the values of control inputs which are used in the process of automatic control of the helicopter are computed.

The linear helicopter model needed for the LQR methodology was developed by global linearization of a full nonlinear model for helicopter hover conditions. This was done numerically within a FLIGHTLAB software resulting the state matrix for 35 state variables and the control matrix for 35 state variables and 4 control variables. Some of the states in the helicopter model are not related to the fuselage dynamic directly (for instance inflow states in aerodynamic loads model), so the sensitivity analysis was done to assess the influence of each state on the control efficiency. As a result, the linear helicopter model containing 21 state variables and 4 control variables was used for LQR.

Therefore, state matrix A for LQR has dimensions (21×21) and contains the following state variables:

- Fuselage (12) – helicopter position in the inertial coordinate system (3), body coordinate system velocities (3), roll, pitch and yaw angles (3), roll, pitch and yaw rates (3),
- Main rotor (9) – induced velocity (3) – 0th harmonic, 1st harmonic (cos), 1st harmonic (sine), each blade flap (3), each blade lag (3).

All four control variables are used, so the control matrix B has dimensions (21×4) . The reduction of matrices dimensions was implemented to diminish computation time, as the method is planned to be implemented at least in a flight simulator operating in real time.

Here, it is assumed that online available state variables data from the sensors are:

- helicopter position in the inertial coordinate system (3),
- helicopter roll, pitch and yaw angles (3),
- helicopter velocities in the body coordinate system (3),
- helicopter roll, pitch and yaw rates (3).

The rest of the states (main rotor induced velocity components, each blade flapping angles, each blade lag angles) are included in the linear model as uncontrolled variables, but

they affect generating the LQR gain matrix K . As these states are not measurable or controllable, the elements of the weight matrix Q related to these states are set to zero.

As a result, the state weight matrix Q is diagonal and has dimensions (21×21) where elements are designated to:

- $Q(1,1)$, $Q(2,2)$, $Q(3,3)$ the position of the helicopter in the inertial coordinate system,
- $Q(4,4)$, $Q(5,5)$, $Q(6,6)$ body coordinate system velocities,
- $Q(7,7)$, $Q(8,8)$, $Q(9,9)$ roll, pitch and yaw angles,
- $Q(10,10)$, $Q(11,11)$, $Q(12,12)$ roll, pitch and yaw rates,
- $Q(13,13)$, $Q(14,14)$, $Q(15,15)$ the 0th harmonic, 1st harmonic (cos) and 1st harmonic (sine) element of the induced velocity,
- $Q(16,16)$, $Q(17,17)$, $Q(18,18)$ each blade flapping angle,
- $Q(19,19)$, $Q(20,20)$, $Q(21,21)$ reflect the regulation of each blade lag.

The control weight matrix R has dimensions (4×4) and diagonal character where the matrix elements are assigned to:

- $R(1,1)$ main rotor lateral cyclic,
- $R(2,2)$ main rotor longitudinal cyclic,
- $R(3,3)$ main rotor collective,
- $R(4,4)$ tail rotor collective.

Effective operation of the LQR depends on the selection of weight matrices. These matrices were calculated here using the iterative expert method. Each of the elements of the Q and R matrices was iteratively adjusted until helicopter responses to control were adequate for the tasks and constraints reflecting the mission.

B. PREDICTION OF VESSEL MOTION

The vessel position and attitude are predicted using the autoregressive method for the time series of past positions and attitudes of the ship. The algorithm collects N samples of components of vessel motion and predicts the motion for the assumed number L of time moments in future. The algorithm works online in a recursive loop: after first collection of the full data set and first complete prediction, it repeats prediction for each new data point entering the system. The discrete autoregressive method with parameters calculated using Burg's method [28] was used, which is described by the equation:

$$x_{N+L} = - \sum_{i=1}^{N-1} a_i x_{N+L-i} \tag{7}$$

where:

- N is the number of the measured samples from the past,
- L is the current number of the predicted sample,
- a_i are the model (autoregressive) parameters calculated using Burg's method,
- x_{N+L-i} are samples which are used as input to the autoregressive model from the last N samples; the model is recursive – in the first step of the algorithm operation, only measured data are used (the first N samples),

in each next step also the predicted samples from previous steps are included in the input of the algorithm (the last N samples).

In Burg's method, model (autoregressive) parameters a_i for a selected autoregressive order $k = N - 1$ are determined by minimizing the total sum of the square of the difference between the original and forward linear prediction values and the square of the difference between the original and backward linear prediction values. The recursive formula for the determining of the parameters a_i is described by the equation:

$$a'_i = a_i + \mu a_{k+1-i} \tag{8}$$

where reflection coefficient μ is described by the equation:

$$\mu = \frac{-2 \sum_{n=0}^{N-k-1} f_k(n+k+1)b_k(n)}{\sum_{n=k+1}^N f_k(n)^2 + \sum_{n=0}^{N-k-1} b_k(n)^2} \tag{9}$$

where:

$$f_k(n) = \sum_{i=0}^k a_i x_{n-i} \tag{10}$$

$$b_k(n) = \sum_{i=0}^k a_i x_{n+i} \tag{11}$$

A complete description of the methodology is presented in [28].

V. MODELING OF VESSEL MOTION

A realistic simulation of vessel motion is important for evaluating both efficiency of the method for prediction of vessels motion and efficiency of the control algorithm in varying environment. The vessel model development was strongly focused on the analysis of selected vessel (frigate) dynamics in waves to obtain response amplitudes of positions and attitudes of the vessel deck.

The vessel motion is modeled using harmonics describing its position and attitude in time.

Calculations were based on Response Amplitude Operators (RAO), which describe response of the vessel to regular wave excitation:

$$RAO(\omega) = \frac{U_A(\omega)}{\xi_A} \tag{12}$$

where:

- $U_A(\omega)$ is the amplitude of vessel response (response here is position or attitude) to regular wave of ω frequency,
- ξ_A is the regular wave amplitude.

The numerical model of the vessel was implemented to the FLIGHTLAB software.

VI. SYSTEM SIMULATION RESULTS

Simulations described in this chapter were performed to validate operation of the algorithms developed and to prove applicability of the methodology and the models for the simulator. This approach is widely used in flight dynamics task in order to limit flight campaign costs [29].

Before the control system tests were performed, the dynamic model of the controlled helicopter was validated

TABLE 1. Test cases – prediction algorithm.

Test no.	Vessel forward velocity [feet/s]	Sea state	Wave heading [deg]
1	33.75	3	180
2		5	

against flight test data and the helicopter responses for control inputs were computed to evaluate requirements for the control algorithm.

The tests presented here focused on validation of:

- prediction of vessel deck motion,
- operation of the integrated control system (helicopter/sensor/automatic control/prediction of vessel deck motion) for selected missions.

The results are described in the following chapters.

A. PREDICTION OF VESSEL MOTION

The prediction algorithm is used to calculate the future vessel deck movement for control purposes. Tests of the prediction algorithm were performed using the model of vessel motion presented above to validate prediction of the future vessel position and attitude.

The data of the vessel deck center point position and attitude were collected for 120 seconds in 1 second intervals. The algorithm predicted the vessel position and attitude for the subsequent 20 seconds.

The simulation tests presented here cover the following cases (Table 1):

- vessel constant forward velocity of 20 knots,
- wave heading 180° (head waves).
- two sea states (in Douglas sea scale):
 - sea state 3 (average wave height 2.87 feet, peak period 6.3 s),
 - sea state 5 (average wave height 10.66 feet, peak period 8.4 s).

The results of simulations are presented in Fig. 3 and Fig. 4. The quality of prediction of the vessel deck position and attitude up to 10 seconds is very good, as differences between the actual and predicted positions are less than 0.5 feet (0.15 m), and the difference between the actual and predicted attitude angle is always less than 0.1 deg.

It seems that the results of prediction of landing deck motion may be used as reliable information for taking the decision to begin the final landing maneuver within 10 seconds.

B. CONTROL SYSTEM OPERATION

In this chapter results of the simulations are presented to illustrate the efficiency of the developed control methodology. It should be noted that simulations reflect total system operation, i.e., the helicopter and the control system dynamics and the automatic control algorithm which uses the algorithm

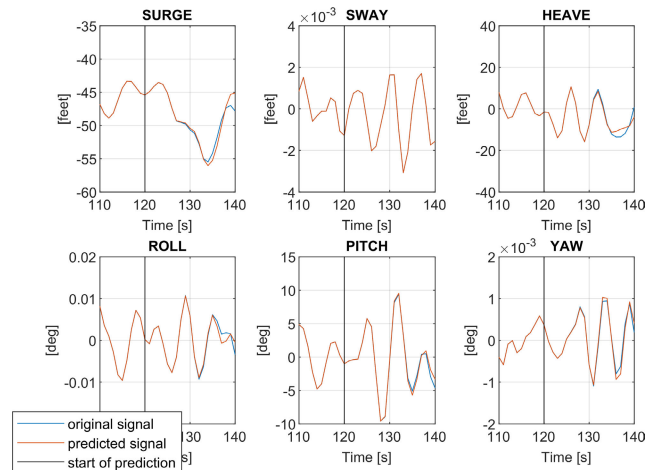


FIGURE 3. Vessel motion prediction – test 1 – sea state 3.

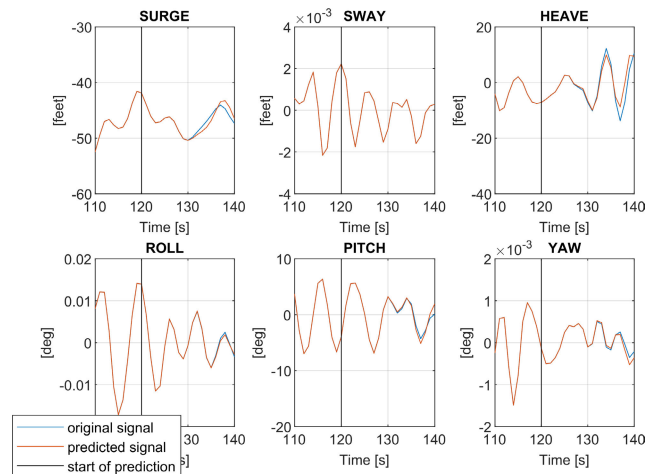


FIGURE 4. Vessel motion prediction – test 2 – sea state 5.

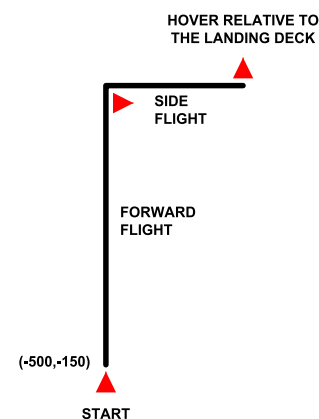


FIGURE 5. Approach steps (horizontal position) related to vessel position in the inertial coordinate system [feet].

predicting the vessel motion. The availability of a set of realistic input data is justified.

The frequently performed procedure (fore/aft procedure [24]) was selected for simulations in this test (Fig. 5). The helicopter flight is decomposed into subsequent phases:

TABLE 2. Test cases – integrated system.

No / Figure	Vessel's forward velocity [feet/s]	Sea state	Wave heading [deg]	Wind speed [feet/s]	Wind heading [deg]
1 / Fig. 6 – Fig. 8	33.75	3	180	21.98 + gusts	180
2 / Fig. 9 – Fig. 11		5		40.35 + gusts	

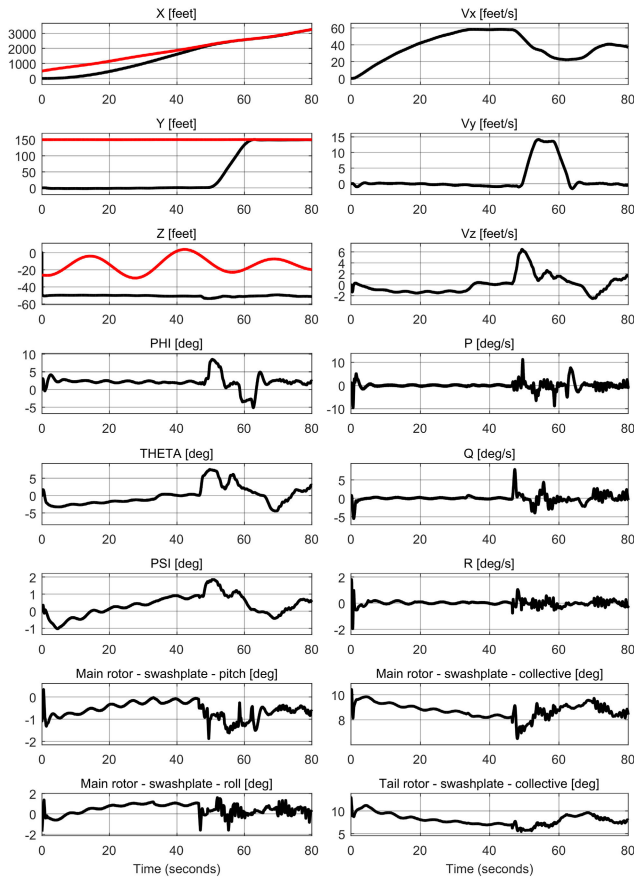


FIGURE 6. Case 1 – approach to the vessel.

- starting from a selected point on the left or right side behind the vessel, forward flight with assumed safe forward velocity at a constant altitude,
- sideward flight with assumed safe side velocity at a constant altitude to take a position over the center point of the vessel landing area,
- hovering relative to the vessel, waiting for the moment when, according to the vessel motion predictions, the touchdown may be performed safely, i.e., the deck will not hit the helicopter during its descent and the deck attitude angles will not exceed the allowable values during the touchdown,
- final landing and deck touchdown.

The simulations results presented here were done for (see Table 2):

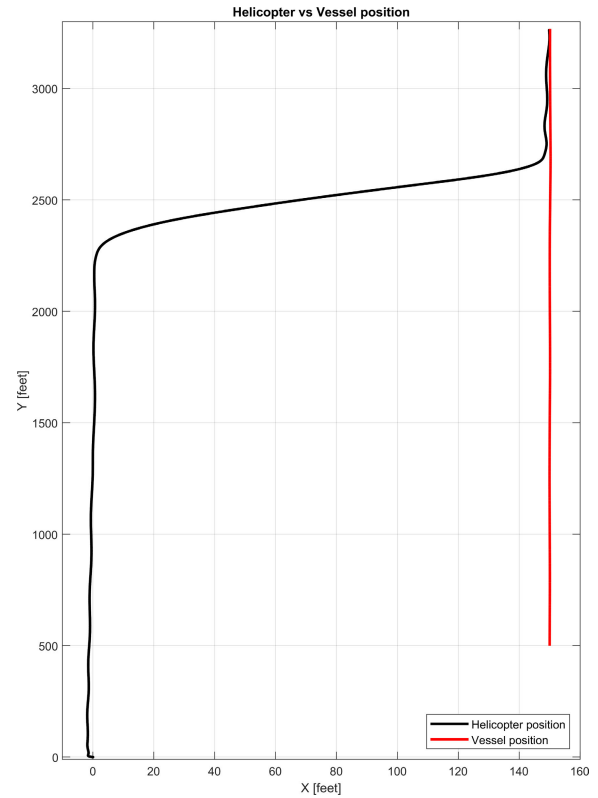


FIGURE 7. Case 1 – approach to the vessel – horizontal position.

- one vessel forward velocity – 20 knots (33.75 feet/s), which is a mean velocity for the selected type of vessel (frigate) during helicopter landing operations,
- one vessel azimuth – 0°,
- two sea states (in Douglas sea scale):
 - sea state 3 (average wave height 2.87 feet, peak period 6.3 s),
 - sea state 5 (average wave height 10.66 feet, peak period 8.4 s),
- one wave heading – 180° (head waves – incoming to the bow),
- two constant wind speeds (in Beaufort scale related to sea state) were included: 21.98 feet/s for sea state 3 and 40.35 feet/s for sea state 5. The system may include wind gusts and turbulence, which were modeled here as sinusoidal variations of the wind speed. In test cases, gusts were applied always when constant wind speed was applied. Gusts were acting in two directions with an amplitude of 20% of the applied constant wind speed v_c :
- head (rear) wind gusts with speed v_x described in time t (s) by equation:

$$v_x = 0.2 * v_c * \sin(t) \tag{13}$$

- side wind gusts with speed v_y described in time t (s) by equation:

$$v_y = 0.2 * v_c * \sin(t) \tag{14}$$

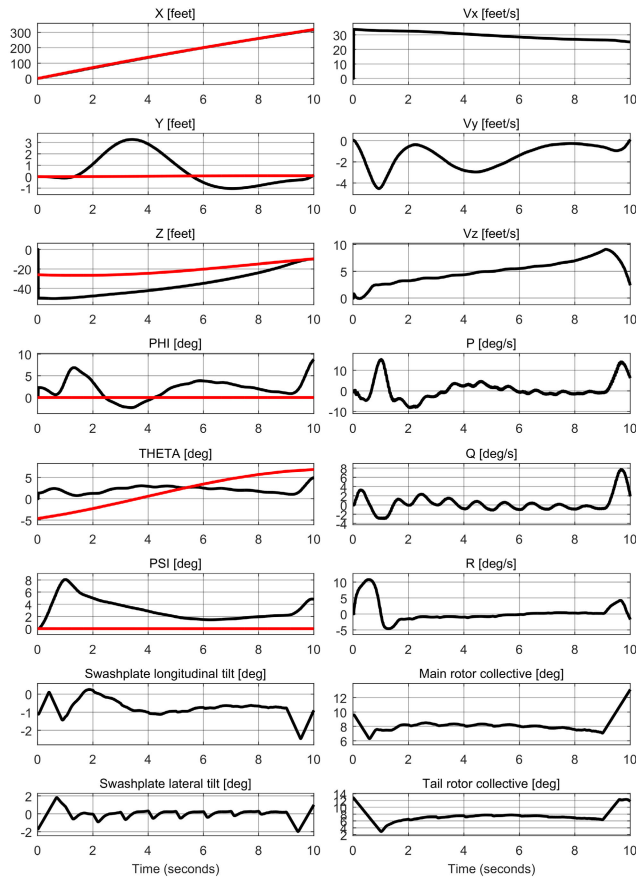


FIGURE 8. Case 1 – landing on the vessel deck.

- one wind heading – 180° (head wind – incoming to the bow).

Each of the tests was divided into two parts:

- approach,
- final landing.

Each of the maneuvers started from a position at 500 feet from the center of the vessel landing area (to stern) and 150 feet from the center point of the landing area (to port).

The simulation results are plotted in Fig. 6 – Fig. 11, where the helicopter responses are marked black and the responses of the vessel – red. Three groups of figures are presented – helicopter responses during the approach to the vessel, helicopter horizontal position changes during the approach to the vessel and responses of the helicopter while landing on the vessel deck.

Responses of the helicopter cover position (X, Y, Z in the inertial coordinate system), attitude (PHI, THETA, PSI in the gravitational coordinate system), linear velocities (Vx, Vy, Vz in the body coordinate system), angular velocities (P, Q, R in the body coordinate system) and values of control variables.

Simulations of the landing phase are terminated 10 seconds from the command to start the landing maneuver, to present the differences in the state variables of the helicopter and

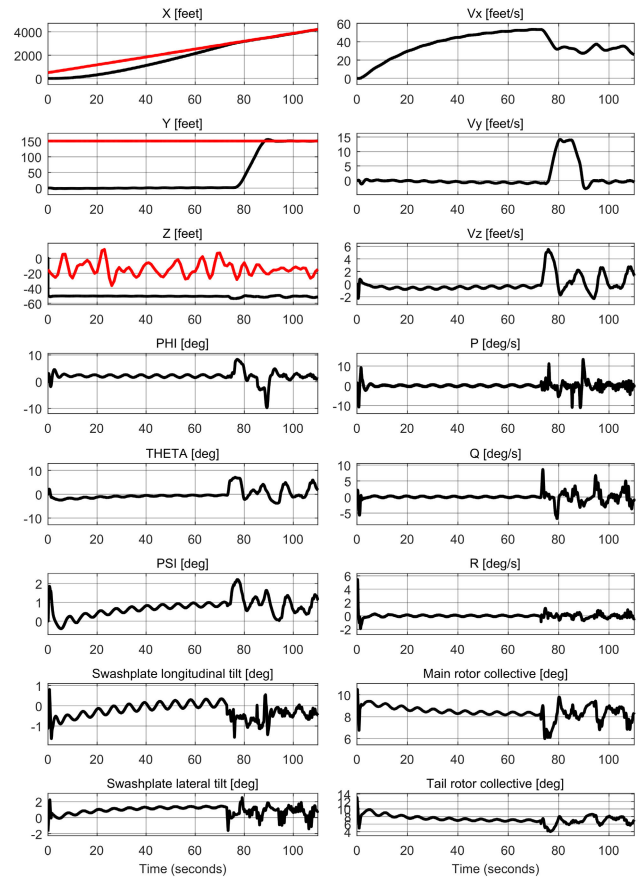


FIGURE 9. Case 2 – approach to the vessel.

- Case 1 (Fig. 6 – Fig. 8)

The case reflects an approach and landing on the moving vessel (sea state 3, head waves), with wind (21.98 feet/s, head wind with gusts). It illustrates the efficiency of the control system when the helicopter is following the vessel, with disturbances from the environment acting on the vessel (velocity and attitude due to the waving changing in time) and on the helicopter (wind and gusts disturbing the helicopter motion).

Results of the approach are presented in Fig. 6 and Fig. 7.

In the approach phase, the attitude of the helicopter was varying in time due to the wind gusts. The control input values also varied in time to stabilize the attitude of the helicopter.

The result of the control is positive because it led the helicopter to achieve and keep the desired position over the landing deck following the (varying in time) velocity of the vessel and successfully compensating for the influence of the head wind and gusts.

Results of the landing maneuver are presented in Fig. 8. The landing was successful – the touchdown was made in ten seconds, deviations in the desired and actual landing position were less than 1.5 feet, attitude angles during the touchdown

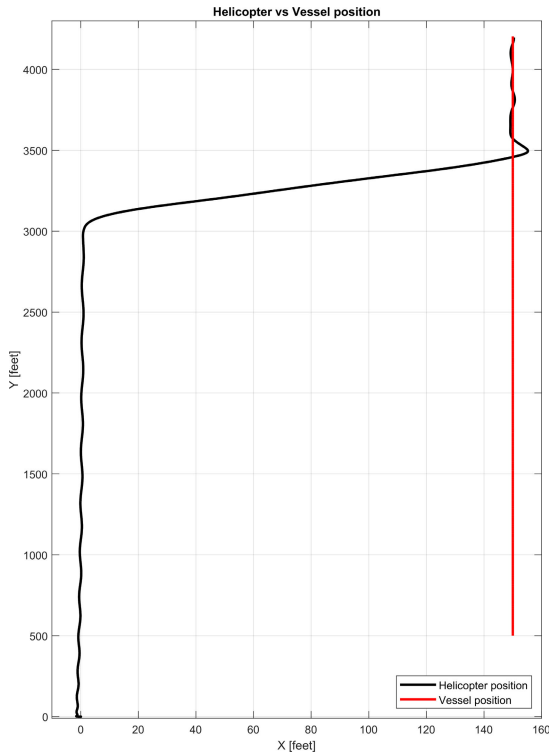


FIGURE 10. Case 2 – approach to the vessel – horizontal position.

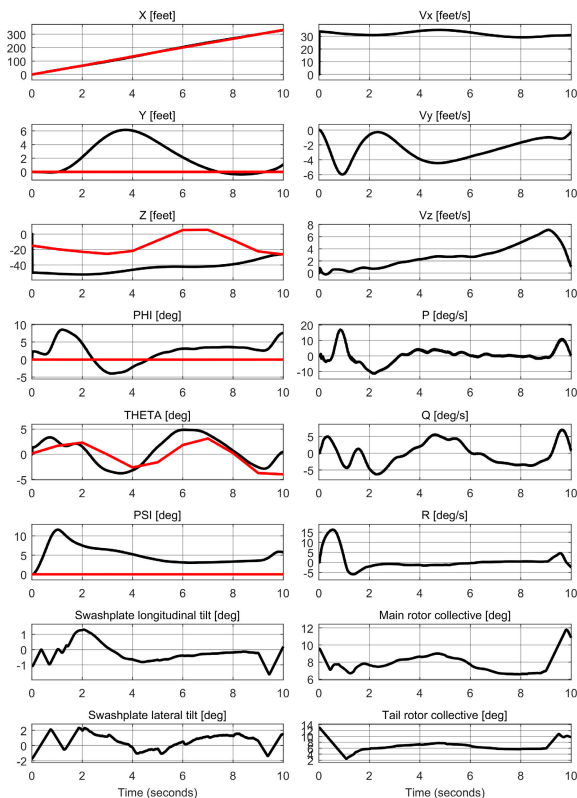


FIGURE 11. Case 2 – landing on the vessel deck.

were small except the roll angle which remained at the level of 8 degrees.

- Case 2 (Fig. 9 – Fig. 11)

The case reflects an approach and landing on the moving vessel (sea state 5, head waves), with wind (40.35 feet/s, head wind with gusts).

Results of the approach are presented in Fig. 9 and Fig. 10.

In the approach phase, due to the strong head wind, responses of the helicopter to the wind gusts were similar to wind disturbances – their sinusoidal character can be clearly seen.

The control efficiency is good because it led the helicopter to achieve and keep the desired position over the landing deck following the (varying in time) velocity of the vessel and successfully compensating for the influence of the head wind and gusts.

Results of the landing maneuver are presented in Fig. 11. Successful landing was performed – the touchdown was made in ten seconds, deviations from the desired landing position were less than 2 feet, attitude angles during the touchdown were small except the roll angle which remained at the level of 8 degrees.

VII. CONCLUSIONS

As preparation for implementation in simulator and prospective hardware tests, the paper presents development and testing of the helicopter automatic control system dedicated to landing on confined and moving surfaces. The validated by flight test data comprehensive model of helicopter and control system dynamics was developed in the FLIGHTLAB environment and used for implementing the novel control algorithm based on LQR control with predicting motion of the landing area.

The simulated helicopter flight was composed of three phases: approach to the landing deck, hovering above it, and final landing with touchdown. In all phases the control was done by the LQR method, adjusted to helicopter type. For safe final landing, the autoregressive method for prediction of future vessel motion was applied. Implementation of the method for the automatic control of the helicopter was described. Landing on a moving vessel deck was the leading example illustrating the efficiency of the methodology. Extensive simulations in various environmental conditions confirmed the efficiency of the developed control methodology.

The general conclusion of the study is that the efficient LQR methodology may be based on simplified system model with carefully selected states and controls.

The continuation of this study will have several stages. First the controlled model will be implemented in a simulator to be assessed by pilots. This will allow to tune the control algorithm to be acceptable also for a human operator on-board. Meantime the models of the control inputs data disturbances will be investigated to define needs for prospective filtering of the sensor data.

The efficiency of the prediction algorithm of a vessel motion will be more carefully investigated for real deck motions data and prospective prediction improvements.

REFERENCES

- [1] W. K. Holmes and J. W. Langelaan, "Autonomous ship-board landing using monocular vision," in *Proc. AHS 72nd Annu. Forum*, West Palm Beach, FL, USA, May 2016, pp. 1–15.
- [2] J. F. Horn and D. O. Bridges, "A model following controller optimized for gust rejection during shipboard operations," in *Proc. Amer. Helicopter Soc. 63rd Annu. Forum*, Virginia Beach, VA, USA, May 2007, pp. 1–14.
- [3] B. Grocholsky, P. DeFranco, H. Cover, A. Singh, and S. Singh, "Robust autonomous ship deck landing for rotorcraft," in *Proc. AHS 72nd Annu. Forum*, West Palm Beach, FL, USA, May 2016, pp. 1–4.
- [4] A. T. McCallum, R. Buchanan, and I. Woodrow, "Modelling of an autonomous MUAV at the ship dynamic interface with a multinational simulation framework," in *Proc. 28th Eur. Rotorcraft Forum*, Bristol, U.K., Sep. 2002, pp. 1–12.
- [5] C. K. Fourie, "The autonomous landing of an unmanned helicopter on a moving platform," M.S. thesis, Stellenbosch Univ., Stellenbosch, South Africa, 2015.
- [6] T. D. Ngo, "Constrained control for helicopter shipboard operations and Moored ocean current turbine flight control," Ph.D. dissertation, Virginia Polytech. Inst. State Univ., Blacksburg, VA, USA, Mar. 2016.
- [7] T. Oktay and C. Sultan, "Constrained predictive control of helicopters," *Aircr. Eng. Aerosp. Technol.*, vol. 85, no. 1 pp. 32–47, 2013.
- [8] B. Ferrier, B. Langlois, F. Bergeron, C. Reboulet, V. Fuertes, and J.-C. Barral, "The design and test using simulation techniques of an automated UAV," in *Proc. AHS 54th Annu. Forum*, Washington, DC, USA, 1998, pp. 1381–1393.
- [9] S. Saripalli, J. F. Montgomery, and G. S. Sukhatme, "Vision-based autonomous landing of an unmanned aerial vehicle," in *Proc. IEEE Int. Conf. Robot. Automat.*, Washington, DC, USA, May 2002, pp. 2799–2804.
- [10] L. A. Sandino, M. Bejar, and A. Ollero, "On the applicability of linear control techniques for autonomous landing of helicopters on the deck of a ship," in *Proc. IEEE Int. Conf. Mechatronics*, Istanbul, Turkey, Apr. 2011, pp. 363–368.
- [11] R. Bradley and G. Turner, "Simulation of the human pilot applied at the helicopter/ship dynamic interface," in *Proc. AHS 55th Annu. Forum*, Montreal, QC, Canada, May 1999, pp. 677–688.
- [12] M. Voskuil, G. D. Padfield, D. J. Walker, B. J. Manimala, and A. W. Gubbels, "Simulation of automatic helicopter deck landings using nature inspired flight control," *Aeronaut. J.*, vol. 114, no. 1151, pp. 25–34, Jan. 2010.
- [13] T. Strohmaier, R. Lantsch, and S. Greiser, "Assisted landing for helicopters in confined areas," in *Proc. 36th Eur. Rotorcraft Forum*, Paris, France, Sep. 2010, pp. 1–12.
- [14] S. Scherer, L. Chamberlain, and S. Singh, "Autonomous landing at unprepared sites by a full-scale helicopter," *Robot. Auton. Syst.*, vol. 60, no. 12, pp. 1545–1562, Dec. 2012.
- [15] S. Saripalli and G. S. Sukhatme, "Landing a helicopter on a moving target," in *Proc. IEEE Int. Conf. Robot. Automat.*, Roma, Italy, Apr. 2007, pp. 2030–2035.
- [16] W. Bagen, J. Hu, and Y. Xu, "A vision-based unmanned helicopter ship board landing system," in *Proc. 2nd Int. Congr. Image Signal Process.*, Tianjin, China, Oct. 2009, pp. 1–5.
- [17] V. Comandur and J. V. R. Prasad, "Rotorcraft shipboard landing guidance using MPPI trajectory optimization," in *Proc. 44th Eur. Rotorcraft Forum*, Delft, The Netherlands, Sep. 2018, pp. 1–4.
- [18] J. V. R. Prasad, V. Comandur, R. Walters, and D. Guerrero, "Model predictive path integral approach for trajectory guidance of rotorcraft shipboard landing," in *Proc. AHS 74th Annu. Forum*, Phoenix, AZ, USA, May 2018, p. 1.
- [19] *Anonymous, Out of the Box: Ideas About the Future of Air Transport. Part 2*, Eur. Commission, Brussels, Belgium, Nov. 2007.
- [20] M. Jump, G. D. Padfield, M. D. White, P. Fua, J.-C. Zufferey, F. Schill, R. Siegart, S. Bouabdallah, M. Decker, J. Schippl, M. Höfing, F. M. Nieuwenhuizen, and H. H. Bühlhoff, "myCopter: Enabling technologies for personal air transport systems," in *Proc. RAEs Conf. Future Rotorcraft*, London, U.K., Jun. 2011, pp. 1–15.
- [21] M. Jump, P. Perfect, G. D. Padfield, M. White, D. Floreano, P. Fua, J.-C. Zufferey, F. Schill, R. Siegart, S. Bouabdallah, M. Decker, J. Schippl, S. Meyer, M. Höfing, F. M. Nieuwenhuizen, and H. H. Bühlhoff, "myCopter: Enabling technologies for personal air transport systems—An early progress report," in *Proc. 37th Eur. Rotorcraft Forum*, Gallarate, Italy, Sep. 2011, pp. 1–12.
- [22] P. Perfect, M. Jump, and M. White, "Development of handling qualities requirements for a personal aerial vehicle," in *Proc. 38th Eur. Rotorcraft Forum*, Amsterdam, The Netherlands, Sep. 2012, pp. 1–18.
- [23] R. Du Val and C. He, "FLIGHTLAB modeling for real-time simulation applications," *Int. J. Model., Simul., Sci. Comput.*, vol. 8, no. 4, 2017, Art. no. 1743003.
- [24] *Helicopter/Ship Qualification Testing, RTO AGARDograph 300 Flight Test Techniques Series—Volume 22*, NATO Res. Technol. Org., France, 2003.
- [25] B. Ferrier, P. Crossland, A. T. McCallum, and A. Manning, "Simulation techniques in the design and test of a recovery phase solution for an automated VTOL-UAV shipboard recovery system," in *Proc. Amer. Helicopter Soc. 58th Annu. Forum*, 2002, pp. 1481–1488.
- [26] S. Arora, S. Jain, S. Scherer, S. Nuske, L. Chamberlain, and S. Singh, "Infrastructure-free shipdeck tracking for autonomous landing," in *Proc. IEEE Int. Conf. Robot. Automat.*, Karlsruhe, Germany, May 2013, pp. 323–330.
- [27] F. Dul, P. Lichota, and A. Rusowicz, "Generalized linear quadratic control for a full tracking problem in aviation," *Sensors*, vol. 20, no. 10, p. 2955, 2020.
- [28] C. Collomb, "Burg's method, algorithm and recursion," Tech. Rep., Nov. 2009. [Online]. Available: <http://www.emptyloop.com/technotes/A%20tutorial%20on%20Burg%27s%20method,%20algorithm%20and%20recursion.pdf>
- [29] P. Lichota, J. Szulczyk, M. B. Tischler, and T. Berger, "Frequency responses identification from multi-axis maneuver with simultaneous multisine inputs," *J. Guid., Control, Dyn.*, vol. 42, no. 11, pp. 2550–2556, Nov. 2019.



SEBASTIAN TOPCZEWSKI received the Ph.D. degree in automation from the Warsaw University of Technology (WUT), in 2019. He is currently an Assistant Professor with the Division of Automation and Aeronautical Systems, Faculty of Power and Aeronautical Engineering, WUT. His research interests include aircraft supervision systems, avionics, navigation, and control systems.



JANUSZ NARKIEWICZ has been a Full Professor, since 2007, and the Head of the Division of Automation and Aeronautical Systems, Faculty of Power and Aeronautical Engineering, Warsaw University of Technology. His current research interests include computer modeling and simulation, avionics, control and navigation systems, rotary wing aeromechanics, and space vehicles.



PRZEMYSŁAW BIBIK received the Ph.D. degree in aerospace engineering from the Warsaw University of Technology. Since 2007, he has been working with the Division of Automation and Aeronautical Systems, Faculty of Power and Aeronautical Engineering, Warsaw University of Technology. His research interests include rotorcraft and unmanned systems modeling and simulation.